X-ray bandwidth: Determination by on-edge absorption and effect on various absorption experiments

Martin D. de Jonge, Zwi Barnea, Chanh Q. Tran, and Christopher T. Chantler*
School of Physics, University of Melbourne, Australia
(Received 2 October 2003; published 27 February 2004)

Knowledge of the monochromaticity of an x-ray source is increasingly important in fundamental experiments and critical applications. The bandwidth of an x-ray beam, selected from a synchrotron radiation spectrum for example, ultimately defines the limiting resolution of the synchrotron source. The development of x-ray technology through the use of characteristic line sources of fixed line shape has impaired the development of understanding of this parameter. The bandwidth is particularly relevant with the modern trend towards the use of synchrotron sources in conjunction with monochromating devices, where the monochromaticity of the x-ray beam is not known *a priori*. The ability to control the bandwidth of the beam can lead to significant new experiments. We have observed the effect of the x-ray bandwidth on precise but relatively scaled measurements of the mass attenuation coefficient of molybdenum made on the absorption edge. We derive an expression describing the effect of the x-ray bandwidth on these measurements and invert this to determine the bandwidth of a highly monochromatized 20-keV synchrotron x-ray beam to be 1.57 eV$\pm$0.03 eV. The technique presented here determines the bandwidth, a parameter critically dependent on the x-ray optical elements in the beam, in such a manner as to require no knowledge of these elements. We demonstrate that the x-ray bandwidth has significant effects upon measured edge energies, mass attenuation coefficients, x-ray anomalous-fine structure and x-ray absorption near-edge structure (XANES). In particular, the observed x-ray bandwidth necessitates a correction of up to 1.4% in the measurement of the mass attenuation coefficient of molybdenum on the absorption edge and is shown to shift the observed absorption-edge energy location by up to 0.5 eV.

DOI: 10.1103/PhysRevA.69.022717 PACS number(s): 32.80.Cy, 78.20.Ci, 07.85.Qe, 61.10.Ht

I. INTRODUCTION

The spectral bandwidth of an x-ray beam can be a key contributor to limiting resolution in powder diffraction [1], single-crystal diffraction [2] grazing-incidence reflection [3,4], imaging [5,6], and spectroscopic [7–9] experiments. The accurate determination of the bandwidth of an x-ray beam will improve the ability to quantify and correct sources of systematic error which will therefore improve the power of these investigations.

However, due to the history of the development of x-ray technology, ''on-line'' techniques for determining the spectral qualities of x-ray beams have not been fully developed. This has come about in part because the properties of the characteristic line spectra produced by laboratory x-ray sources had been relatively well characterized. These were dominated by the high-intensity characteristic lines and a relatively low-intensity bremsstrahlung background, the estimate of whose contribution was sufficient for most investigations. Moreover, the characteristic lines and their dominance were similar for all sources with the same target, and thus did not need reinvestigation for each experiment. Difficulties resulting from the fact that the characteristic $K\alpha$ line was a doublet provided some limitation [10–13]. Empirical profile fitting of this spectral feature led to a range of spectroscopic issues and to limitations in the accuracy of lattice parameter and structure determination [14–19], but these have generally been accepted as intrinsic limitations of the experimental methods. While methods of robust fitting analysis have developed strongly, they have usually not focussed on interpretation in terms of the intrinsic bandwidth of the x-ray beam.

Diffractive monochromation of characteristic lines to separate the $K\alpha_1$ and $K\alpha_2$ doublet in a particular experiment appeared adequate for most applications, and therefore little further direct investigation of x-ray beam monochromaticity and its impact upon experimental results was undertaken, with some notable exceptions [20–22].

The more recent trend towards the use of tunable synchrotron sources requires careful investigation of the bandwidth of the x-ray beam selected from the synchrotron spectrum in order to identify its effect on the source, crystal, or detector performance directly. Direct investigations of the physical properties of materials, for instance by using grazing incidence reflection from thin films, the study of crystal perfection or mosaicity from diffraction profiles, and investigations of the energy of x-ray anomalous fine structure (XAFS) features and of absorption-edge locations, atomic form factors, and radial electron densities, all require an assessment of the degree of monochromaticity or bandwidth of the x-ray beam and the effect of this upon the relevant experimental parameters.

A common technique for placing an upper bound on the bandwidth of an x-ray beam involves the attribution of the entire width of a diffraction profile measured with a perfect crystal to the bandwidth of the beam [23]. This overestimation can provide information for some applications, but does

*Electronic address: chantler@physics.unimelb.edu.au

not enable proper evaluation of the bandwidth necessary for highly critical experiments.

A more careful diffraction-profile analysis can be used to determine the bandwidth of the beam by isolation of its effect on the shape and width of the measured diffraction profile [24]. However, contributions to the observed widths of diffraction peaks arise from many sources: the crystal, including the intrinsic width of the reflection and effects relating to the crystal size, perfection, mosaicity, alignment, and temperature; the beam, including contributions from the beam bandwidth, angular structure (divergence) and finite collimation. When all of these parameters, each of which depends critically on the optical elements placed in the beam, can be quantified, the measured diffraction profile can be used to determine the bandwidth of the x-ray beam. However, the number, sensitivity, and highly correlated nature of these parameters is such as to render this a complex procedure.

Alternative methods for determining the spectral bandwidth of an x-ray beam include single-photon calorimetry [25], exploitation of the wavelength dependence of Pendellösung fringes [26,27], and the measurement of grazing-incidence x-ray reflection profiles in the neighborhood of the high-energy cutoff [28–30]. However, most of these techniques are currently in various stages of development and suffer from difficulties similar to those of the diffraction profile analysis outlined above. The technique of single-photon calorimetry is an exception in this regard, as it can in principle be used to determine the bandwidth with no knowledge of the size, divergence, etc. of the x-ray beam. However, the need for low photon fluxes to produce the single-photon condition generally requires attenuation of the otherwise optimized beam. This attenuation will generally affect the bandwidth of the beam, thus destroying the integrity of the measured quantity.

Techniques for determining characteristic x-ray linewidths to very high accuracy [31,32] cannot generally be used to determine the bandwidth of a tunable x-ray beam due to the specificity of the design and use of the required equipment. Such precision experiments often require construction of high-resolution, narrow-band apparatus suitable only for use within a limited energy range and in a specific geometrical configuration.

Here we report a technique for determining the bandwidth of an x-ray beam which exploits the rapid variation of the mass attenuation coefficient at the absorption edge. Although this technique has been developed in the context of making an accurate determination of the mass attenuation coefficients of molybdenum, it has a much more general application to synchrotron-based investigations.

The technique described here uses the fact that the effect of the beam bandwidth on the measured mass attenuation coefficient varies with the thickness of the absorber used to make the measurement. We observe the effect of the finite bandwidth of an x-ray beam on the measured mass attenuation coefficients in the neighborhood of an absorption edge and derive an expression which describes the effect of the finite bandwidth of the beam on such measurements. We then show that this expression can be inverted and used to apply a correction to the measured values. The bandwidth is then derived from the differences between measurements of the mass attenuation coefficient made with a number of foil thicknesses. An important advantage of our method is that it requires no knowledge of the configuration of the x-ray optics—which is difficult to establish—and that it characterizes the beam after its passage through slits, optical elements, the monochromator, and after detuning.

II. THE EFFECT OF THE X-RAY BANDWIDTH ON ATTENUATION MEASUREMENTS AT THE ABSORPTION EDGE

The most obvious consequence of having a distribution of energies in the x-ray beam is that instead of measuring the mass attenuation coefficient corresponding to a single x-ray energy, we are measuring the combined attenuation at these energies weighted by the intensity of each x-ray energy component. Furthermore, since each energy component will in general have a different attenuation coefficient, the original distribution of energies in the x-ray beam—the beam energy profile—will change gradually as the beam is attenuated by the foil, with the less attenuated components gradually increasing their relative intensity over the more attenuated components. This change in the beam energy profile results in a decrease in the differential attenuation of the beam as it passes through the foil, and will manifest itself experimentally as a systematic decrease of the total measured mass attenuation coefficient as the foil thickness is increased. The effect of the bandwidth on these measurements is greatest on the absorption edge due to the strong distortion of the beam energy profile provided by the rapidly changing mass attenuation coefficient.

In order to determine the bandwidth of the beam used in these measurements, we calculate the mass attenuation coefficients derived from the measured beam intensities and explicitly include the finite bandwidth of the x-ray beam in the calculation. We assume that the detector efficiencies are constant across the relatively narrow bandwidth of the beam. Thus, beginning with the Beer-Lambert absorption law:

$$\exp\left(-\left[\frac{\mu}{\rho}\right]_{mE_0}\rho t\right)=\frac{I}{I_0}, \tag{1}$$

where I represents the attenuated beam intensity, I_0 the unattenuated beam intensity, ρt the product of density and thickness of the attenuating foil, and $[\mu/\rho]_{mE_0}$ the mass attenuation coefficient of the foil material as measured (subscript m) with a beam whose central energy is E_0. Explicit inclusion of the bandwidth gives

$$\exp\left(-\left[\frac{\mu}{\rho}\right]_{mE_0}\rho t\right)=\frac{\int_0^\infty I dE}{\int_0^\infty I_0 dE}, \tag{2}$$

where I_0 now represents the intensity of the incident beam energy profile at each energy E distributed around the central

energy E_0. The transmitted intensity of the beam energy profile, now represented by I, results from the attenuation of each of the energy components in the incident beam by an amount determined by the 'true' mass attenuation coefficient at each energy E, $[\mu/\rho]_{tE}$. Thus

$$\exp\left(-\left[\frac{\mu}{\rho}\right]_{mE_0}\rho t\right)=\frac{\int_0^\infty I_0 \exp\left(-\left[\frac{\mu}{\rho}\right]_{tE}\rho t\right)dE}{\int_0^\infty I_0 dE}. \quad (3)$$

Defining the normalized incident beam energy profile

$$\tilde{I}_0=\frac{I_0}{\int_0^\infty I_0 dE}, \quad (4)$$

this can be written more simply as

$$\exp\left(-\left[\frac{\mu}{\rho}\right]_{mE_0}\rho t\right)=\int_0^\infty \tilde{I}_0 \exp\left(-\left[\frac{\mu}{\rho}\right]_{tE}\rho t\right)dE. \quad (5)$$

The x-ray bandwidth is determined by inverting Eq. (5) and then using this to apply a correction to the mass attenuation coefficients obtained from measurements made with a number of foils of different thickness. The value for the x-ray bandwidth is determined to be that which, when used to correct for the effect of the bandwidth, minimizes the systematic differences between the measured mass attenuation coefficients obtained with foils of different thickness. In order to use this technique, it is therefore necessary to make measurements of the mass attenuation coefficient using at least two foils of very different thickness.

One cannot determine the effect of bandwidth by comparing the mass attenuation coefficient measured with a given thickness of foil with its theoretically predicted value. While mass attenuation coefficients can be predicted to a precision and accuracy of 1% away from absorption edges, reported variation between measurements and theories indicates that this uncertainty is often severely underestimated [33–36]. Hence both theoretical and experimental sources of uncertainty would directly impact upon the determination of the bandwidth. For measurements on the absorption edge, additional experimental uncertainty in energy calibration has the potential to result in a large error in the mass attenuation coefficient, often reaching 10% in magnitude. The situation is further compounded by effects including shake-up and shake-down resonances [37], electron correlations, and chemical effects, giving rise to XAFS [38–40] and XANES [41,42]. Thus, there are no well-defined experimental or theoretical results suitable for comparison in the neighborhood of the absorption edge.

III. EXPERIMENTAL RESULTS

The results of an experiment designed to determine the mass attenuation coefficients $[\mu/\rho]$ for molybdenum at various energies between 13.5 keV and 41.5 keV are shown in Fig. 1. These results were obtained in a x-ray transmission experiment similar to that reported elsewhere [43]. Figure 1 shows around 600 independent measurements made at 219 energies, with the energy interval between measurements chosen to be commensurate with the expected structure in the mass attenuation coefficient. Thus, approximately half of the measurements have been made within 1 keV of the absorption edge at 20 keV. The measurements presented in this and subsequent figures are highly precise, but have not been determined on an absolute scale. Such a determination requires further input regarding the absolute value of the density and thickness of the absorber used in the measurement, the quantification of the attenuation of the air path, and other factors. The impact of these factors on the measured attenuation is being investigated, and will result in an extensive dataset to be reported in a future article. However, absolutely-scaled measurements are not required to determine the bandwidth, the chief concern of this paper.

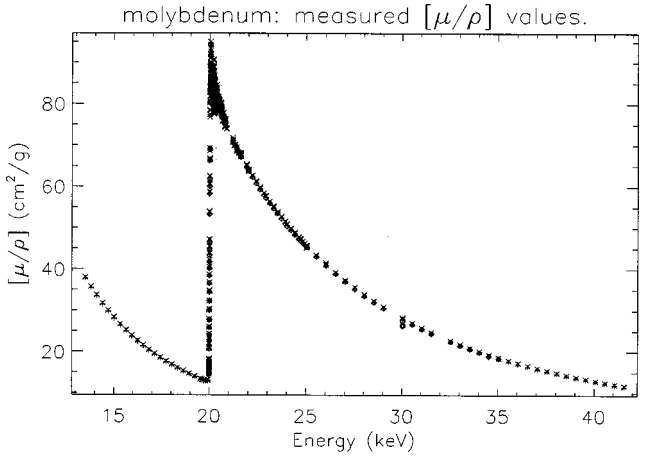

FIG. 1. Results of measurements of the mass attenuation coefficient of molybdenum. At each energy measurements have been made with three thicknesses of foil, spanning a factor of 4 in attenuation, μt, represented by three different symbols: ×—100 μm, +—50 μm, ◇—25 μm. The consistency of the experimental results is too good for the three independent measurements at each energy to be clearly resolved on this scale.

In Fig. 2 we show the values of the measured mass attenuation coefficients in a small range of energies about the absorption edge. These plots depict an increase of the absorption coefficient of molybdenum of 400%–500% over an energy range of 20 eV in the vicinity of the absorption edge at $\approx$20 keV. Additionally, in Fig. 2 we present the numerical derivative of the weighted mean of the measurements at each energy, where the ordinate scale is relative. This curve shows quite clearly the position of the first point of inflection at around 19.995 keV.

The measurements were made at beamline 1-ID of the Advanced Photon Source synchrotron facility at Argonne National Laboratory. The x-ray beam was produced by an undulator insertion device, with the third order of the undulator spectrum tuned to the required experimental energy. This spectrum was monochromated by reflection by the (311) planes of a silicon double-reflection monochromator. The second crystal of this monochromator was detuned

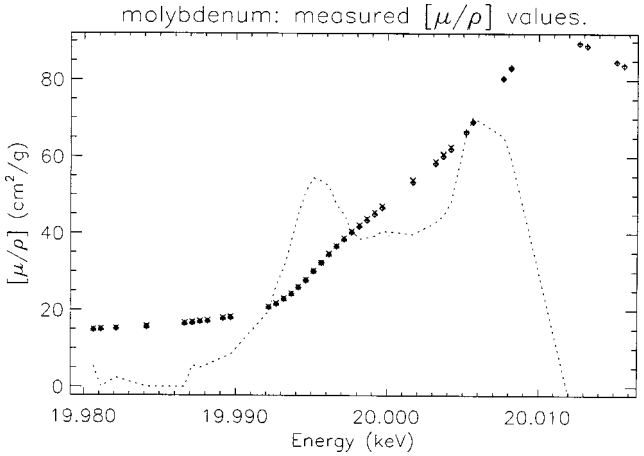

FIG. 2. Results of measurements of the mass attenuation coefficient of molybdenum in the near-edge region. At each energy measurements have been made with three thicknesses of foil, represented by three different symbols: ×—100 μm, +—50 μm, ◇—25 μm. The consistency of the experimental results is too good for the three independent measurements at each energy to be clearly resolved on this scale, although a small trend in the deviation of the thickest foil can be seen. The gradient of the weighted mean of the measurements made at each energy is plotted as a dotted line, on a relative scale.

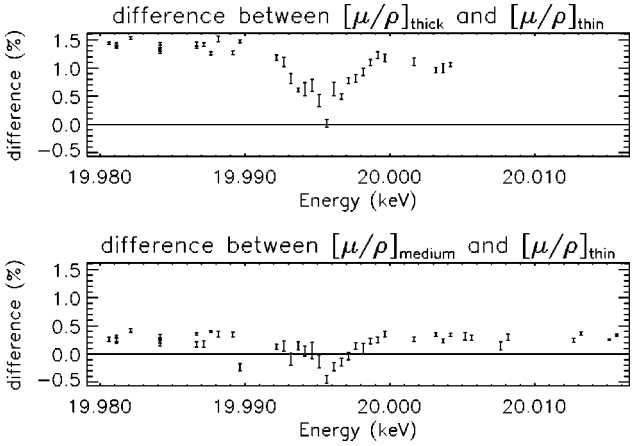

FIG. 3. Percentage differences of the measured mass attenuation coefficients $[\mu/\rho]$ using the thickest (top, 100 μm thick) and medium (bottom, 50 μm thick) foils compared to those made with the thinnest foil (25 μm thick). The error bars represent the $1\sigma_{se}$ deviation of the weighted mean. Explicitly, the ordinate is $100([\mu/\rho]_{thicker}-[\mu/\rho]_{thin})/[\mu/\rho]_{thin}$. Well below the absorption edge, the systematic differences of the thick and medium foil measurements from those of the thin foil, of $\leqslant 1.5\%$ and $\leqslant 0.4\%$ respectively, are due to the use of nominal foil thicknesses.

slightly from the parallel position to suppress the harmonic components of the beam, as discussed elsewhere [44,45].

In making the measurements presented in Figs. 1 and 2, we have used an optimized, automated control sequence to adjust the undulator gap, the monochromator angle, and the detuning of the second element of the double-reflection monochromator in a consistent and reproducible manner. Particular care was taken when adjusting detuning of the second crystal, which is likely to have the largest impact on the stability of the bandwidth of the x-ray beam. The total intensity of x-rays passing through the monochromator was found to be between 35% and 55% of the peak, undetuned intensity for all measurements. There is some fluctuation of the bandwidths of the beams produced in this manner, so we determine the average bandwidth of the beams over a range of energies.

Unlike most previous attenuation measurements (discussed in Refs. [46,47] and compiled in Refs. [48,49]), independent measurements of the mass attenuation coefficients were made for three different foil thicknesses, covering a factor of 4 of attenuation, with $\mu t \approx \{0.25,0.5,1\}$ below the absorption edge, rising to $\mu t \approx \{1.5,3,6\}$ at 20.005 keV. Each measurement was repeated ten times to yield an independent measure of the precision and reproducibility of these measurements [50,51]. These sets of ten identical measurements were repeated at least three times with apertures of various diameters placed between the sample and the ion-chamber detectors to quantify the effects of scattering in a manner similar to that reported elsewhere [43], although with a smaller solid angle subtended to the foil, making the measurements less sensitive to the effect of the scattered photons. As there was no systematic trend of the measurements with the diameter of the aperture, we conclude that the measurements were not affected by scattering and thus present, for clarity in the figures, the weighted mean of the measurements made with each foil. However, the calculation described here was carried out using the unaveraged data.

On the scale of Fig. 2, the results appear to be consistent and the near-edge structure appears to be well determined. The result could clearly be used quantitatively, for example, to report XANES. However, the precision of each measurement is sufficiently good for the discrepancies in the data to be further interpreted. The use of a number of sample thicknesses and of multiple measurements allows the proper determination of the statistical precision of the measurements which enables us to identify the signature of the x-ray beam bandwidth.

The detailed discrepancies and deviations, unresolved in Fig. 2, are revealed in Fig. 3, where we present the percentage differences between the mass attenuation coefficients obtained with the thick and medium foils from those taken with the thin foil. We present the results as the differences between the measurements made with the different foil thicknesses in order to highlight the thickness dependence of the effect of the bandwidth that we wish to exploit. The error bars in this plot represent the standard error (i.e.,one standard deviation of the mean, $1\sigma_{se}$) of the weighted mean of measurements made with each foil added in quadrature to that of the thin foil. In this plot we can see that there is a systematic discrepancy of around 1.5% and 0.4% for the thick and medium foils, respectively, compared with the results obtained with the thinnest foil. This discrepancy is due to the use of the nominal thicknesses of the foils and is completely consistent with the manufacturer's tolerance on the nominal thickness and uniformity of the foils. While these thicknesses can be determined on an absolute scale [52], relative information is sufficient for the bandwidth determination.

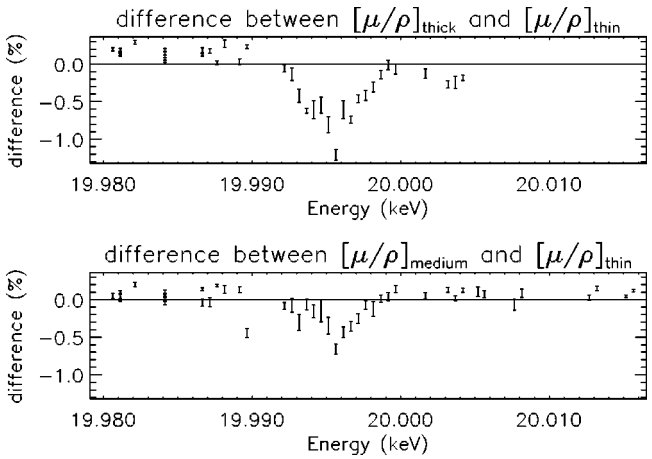

FIG. 4. Percentage difference between the results of the mass attenuation coefficient $[\mu/\rho]$ obtained from measurements made with the thickest (top, 100 μm thick) and medium (bottom, 50 μm thick) foils and those made with the thinnest foil (25 μm thick). The error bars represent the $1\sigma_{se}$ deviation of the weighted mean. The discrepancy due to the incorrect calibration of the foil thicknesses has been removed by fitting the thicknesses of two of the foils to that of the third. The effect of the bandwidth of the x-ray beam is now clearly visible in the form of a prominent deviation which correlates with the gradient of the mass attenuation coefficient, as presented in Fig. 2. As shown in the text, this gradient-correlated deviation, peaking at around 19.995 keV, is the signature of the effect of the bandwidth.

The discrepancies presented in Fig. 3 can be corrected by performing a least-squares fit of the thickness of the two thicker foils relative to that of the third. This has the effect of shifting all the measurements relating to a given foil by the same amount parallel to the ordinate axis. The results of this procedure are presented in Fig. 4, where the ordinate again represents the percentage difference between the results obtained with the thick and medium foils and those of the thin foil, but now after the discrepancies due to the use of the nominal foil thicknesses have been corrected. This correction gives a proper estimate of the relative local foil thickness exposed to the x-ray beam. After this scaling has been carried out, we note a residual trend of deviations which peak at 19.995 keV, where the thicker foils return consistently lower values than those of the thin foil. As we will show, this residual deviation is due entirely to the bandwidth of the beam.

IV. TAYLOR SERIES EXPANSION FOR INVERSION AND BANDWIDTH DETERMINATION

The effect of the beam bandwidth varies with absorber thickness. Discrepancies between measurements made with a variety of foil thicknesses are corrected using a physical model whose input is the bandwidth of the beam. In order to calculate this correction, we must invert Eq. (5). We obtain the correction c_{E_0} to be made to the measured mass attenuation coefficient for each of the foil thicknesses and at each experimental energy E_0,

$$c_{E_0} = \left[\frac{\mu}{\rho}\right]_{tE_0} - \left[\frac{\mu}{\rho}\right]_{mE_0} \tag{6}$$

$$= \left[\frac{\mu}{\rho}\right]_{tE_0} + \frac{1}{\rho \mathrm{t}} \ln\left[\int_0^\infty \tilde{I}_0 \exp\left(-\left[\frac{\mu}{\rho}\right]_{tE} \rho \mathrm{t}\right) dE\right], \tag{7}$$

where we have used Eq. (5). However, Eq. (7) refers to the true mass attenuation coefficient, which is unknown at this stage. To evaluate this expression, we linearize the mass attenuation coefficient about E_0 by means of a Taylor series to give

$$c_{E_0} \approx \left[\frac{\mu}{\rho}\right]_{tE_0} + \frac{1}{\rho \mathrm{t}} \ln\left[\int_0^\infty \tilde{I}_0 \exp\left(-\left[\frac{\mu}{\rho}\right]_{tE_0} \rho \mathrm{t}\right) \times \exp\left(-\frac{d\left[\frac{\mu}{\rho}\right]_{tE_0}}{dE}(E-E_0)\rho \mathrm{t}\right) dE\right] \tag{8}$$

$$= \left[\frac{\mu}{\rho}\right]_{tE_0} + \frac{1}{\rho \mathrm{t}} \ln\left[\exp\left(-\left[\frac{\mu}{\rho}\right]_{tE_0} \rho \mathrm{t}\right) \int_0^\infty \tilde{I}_0 \times \exp\left(-\frac{d\left[\frac{\mu}{\rho}\right]_{tE_0}}{dE}(E-E_0)\rho \mathrm{t}\right) dE\right] \tag{9}$$

$$= \frac{1}{\rho \mathrm{t}} \ln\left[\int_0^\infty \tilde{I}_0 \exp\left(-\frac{d\left[\frac{\mu}{\rho}\right]_{tE_0}}{dE}(E-E_0)\rho \mathrm{t}\right) dE\right]. \tag{10}$$

The validity of this expansion relies on the second-order correction being small,

$$\frac{d^2\left[\frac{\mu}{\rho}\right]_{tE_0}}{d^2E} \frac{(E-E_0)^2}{2} \ll \frac{d\left[\frac{\mu}{\rho}\right]_{tE_0}}{dE}(E-E_0), \tag{11}$$

for the range of energies across the bandwidth. The absorption edge is some 20 eV wide and, as will be seen, the bandwidth is of the order of 1 eV. Hence, although the mass attenuation coefficient is certainly not a linear function of energy, and in fact has a very strong nonlinearity with respect to energy across the absorption edge, nonetheless on the relevant eV scale the deviation from nonlinearity is quite small. Measurements taken in the XAFS region cannot be treated in this manner as they do not satisfy the conditions of the linearized approximation expressed in Eq. (11).

Equation (10) tells us that the correction due to the finite bandwidth of the beam is due, to first order, to the gradient of

the true mass attenuation coefficients, which are not known. However, since the difference between the measured and true values is proportional to the gradient, the difference between their gradients will vary with the curvature. Thus, the true gradient is the same as the measured gradient, to the same order of approximation already used to obtain Eq. (10), which can be recast as

$$c_{E_0} \approx \frac{1}{\rho \mathrm{t}} \ln\left[\int_0^\infty \tilde{I}_0 \exp\left(-\frac{d\left[\frac{\mu}{\rho}\right]_{mE_0}}{dE}(E-E_0)\rho \mathrm{t} \right) dE \right], \tag{12}$$

where the gradient of the measured values of the mass attenuation coefficient has replaced the gradient of the true values. Inaccuracies resulting from the use of the gradient of the measured values have been circumvented by running the correction algorithm in a two-pass manner: the first pass is used to determine an approximate correction from which the gradient is calculated for use in the second-pass correction. The results of these second-pass calculations were consistent with the single-pass results, and thus the use of Eq. (12) was explicitly validated.

Equations (10) and (12) express a first-order dependence of the effect of the x-ray bandwidth on the gradient of the mass attenuation coefficient. The spread of energies in the beam ''sees'' both the value and gradient of the mass attenuation coefficient. The correction term c_{E_0} reveals no dependence on the value of the mass attenuation coefficient, leaving only the gradient term.

Figure 4 shows a consistent trend in the residual deviations between the mass attenuation coefficients obtained with the thicker foils and those of the thin foil. This deviation peaks at 19.995 keV, where the thicker foils return a consistently lower value than that of the thin foil. This deviation increases in proportion to the gradient of the mass attenuation coefficient, as can be seen by comparison with Fig. 2, and is consistent with the effect due to the finite bandwidth of the x-ray beam described by Eq. (12). The effect of the derivative (presented in Fig. 2) on the deviation of the mass attenuation coefficients is suppressed as the mass attenuation coefficient increases due to the presentation of the percentage difference in Fig. 4.

Interestingly, the deviations presented in Fig. 4 correlate uniquely with the gradient of the mass attenuation coefficient presented in Fig. 2, and therefore the cause of the deviations is indeed the finite bandwidth of the beam. This can be seen by realizing that in order for deviations to correlate with the gradient, the gradient must be probed. In order to probe the gradient, there must be a finite spread of energies in the beam, i.e., the beam must have a finite bandwidth.

Given an estimate of the incident beam energy profile $\tilde{I}_0$, we can use Eq. (12) to calculate the correction to the mass attenuation coefficients. Once we have chosen a model beam energy profile, the integral in Eq. (12) can be evaluated by employing appropriate numerical methods. At this stage we assume the beam energy profile to have a Gaussian distribution of width W_{FWHM} around the central energy E_0, and defer discussion of the implications of this assumption until later.

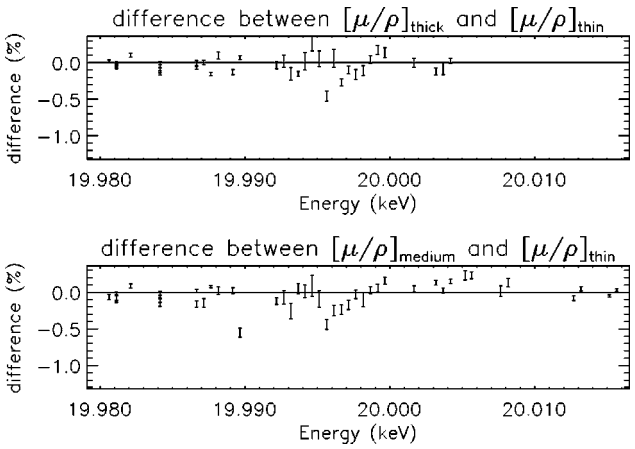

FIG. 5. Percentage differences between the mass attenuation coefficients $[\mu/\rho]$ obtained from measurements made with the thickest (top, 100 μm thick) and medium (bottom, 50 μm thick) foils and those made with the thinnest foil (25 μm thick) after correcting for the effect of the finite bandwidth of the x-ray beam. The prominent, gradient-correlated deviation visible in Fig. 4 has effectively disappeared. The correction for the use of the nominal thicknesses of the foils is also carried out in the calculation, allowing the points to shift parallel to the ordinate axis so that they have a minimum least-squares deviation from the zero line, as before.

We have evaluated the integral by means of a finite sampling of the integrand over a finite energy range. We have parametrized this sampling using two parameters: the range of evaluation of the profile in units of the full width at half maximum (FWHM), r_W, and the sampling frequency in units of the number of sample points within each FWHM, s_{FW}. Thus, Eq. (12) is evaluated from

$$c_{E_0} = \frac{1}{\rho \mathrm{t}} \ln\left[\sum_{k=-j}^{j} \tilde{I}_0(E_0 + k\Delta E) \times \exp\left(-\frac{d\left[\frac{\mu}{\rho}\right]_{m,E_0}}{dE}(k\Delta E)\rho \mathrm{t} \right) \right], \tag{13a}$$

$$j = \frac{r_W(s_{FW}-1)}{2}, \quad \Delta E = \frac{W_{FWHM}}{s_{FW}-1}, \tag{13b}$$

$$s_{FW} \in \text{odd integers}, \tag{13c}$$

where, by forcing s_{FW} to be odd we ensure that the dominant, central contribution from the beam energy profile is evaluated.

The parameters involved in this process (sampling frequency s_{FW} and range r_W) were tested and found to produce robust and well-converging results. The derivative in the summation is evaluated by determining the numerical derivatives of the weighted mean of the measured mass attenuation

coefficients, achieved by using the three-point Lagrangian interpolation algorithm of Hildebrand [53].

Results of the minimization of the deviations are presented in Fig. 5. A comparison of Fig. 4 with Fig. 5 shows that the magnitude of the deviations between the measurements in the region 19.99 keV$<E<$20 keV have been significantly reduced.

The value of the average FWHM bandwidth W_{FWHM} of the x-ray beam that minimizes the discrepancies is 1.57 eV ± 0.03 eV, assuming a Gaussian distribution of energies. The error attributed to the bandwidth comes from the fitted one standard deviation error estimate multiplied by the square root of the reduced chi squared $\sqrt{\chi_r^2}$, thus assuming that the inadequacies of the estimated input uncertainties do not invalidate the functional approach.

The determined value for the average bandwidth of the beam is not inconsistent with the official figure for the monochromaticity of the x-ray beam at beamline 1-ID, $\delta E/E = 10^{-4}$, giving a bandwidth of $\Delta E = (\delta E/E)E = 10^{-4} \times 20$ keV$=2$ eV. The latter nominal bandwidth is quoted by many synchrotron radiation facilities employing silicon double-reflection monochromators, and is a rough estimate of the bandpass of this type of monochromator. The monochromaticity of synchrotron beams has not been better characterized because, as discussed earlier, such a measurement is usually very difficult to accomplish.

The χ_r^2 provides a measure of the improvement of the consistency of the determined mass attenuation coefficients after the bandwidth correction. The χ_r^2 associated with the measurements before and after the bandwidth correction, as presented in Figs. 4 and 5, has decreased from 7.8 to 4.5, clearly confirming the presence and successful correction of this effect.

The χ_r^2 over the reduced dataset is greater than 1 after correcting for the effect of the bandwidth. This indicates a limitation of either the input values of the fit, the uncertainty estimates for these values, or the assumptions of the model employed. In our case, the nonunitarity of χ_r^2 is primarily due to the assumption that a single value of the bandwidth of the beam can be used to correct all of the measured mass attenuation coefficients. In the approach presented here, a single *average* bandwidth is determined by fitting to the entire dataset. Despite the experimental aim to maintain a constant bandwidth, the x-ray bandwidth did in fact vary. The variation of the x-ray bandwidth contributes to the residual discrepancies of the corrected values on the absorption edge, where the effect of the bandwidth is greatest, as observed in Fig. 5, compared with those well away from the edge, where the effect of the bandwidth is insignificant. The weak, systematic structure that can be observed in the residual discrepancies in Fig. 5 correlates with a similar pattern in the detuning of the beam, and hence probably represents a real variation of the bandwidth of the beam.

V. CONVERGENCE, STABILITY, AND ROBUSTNESS OF THE TECHNIQUE

A. Truncation and filtering of the data

As mentioned, this work has arisen from the measurement of the mass attenuation coefficients of molybdenum over a wide range of energies. In this wide survey, we have developed techniques for testing for the presence of systematic errors due to harmonic components in the beam, fluorescent, Rayleigh, and Compton scattering, incorrectly determined zero-beam count rates, and the bandwidth of the x-ray beam, and for correcting the effects of these systematic errors when present in the measured data.

By contrast, the effect of the bandwidth on the mass attenuation coefficients is only significant over a very narrow range of energies at the absorption edge. For example, when the entire dataset is subjected to the correction algorithm, a correction greater than 0.1% is required for measurements made at only 24 out of a total of 219 experimental energies. The use of measurements at all 219 energies would therefore decrease the reliability of the bandwidth determination due to domination by the random and systematic errors which, in all but 24 measurements, would probably exceed the magnitude of the negligible bandwidth effect. Accordingly, in deriving the bandwidth we have reduced the scope of the data used in the fitting process to the range of energies around the absorption edge, extending from 19.980 keV to 20.015 keV, in which the bandwidth effect is most pronounced.

We have also discarded measurements for which $\mu t > 6$, these being affected by harmonic contributions and background zero-beam noise. Likewise, we have discarded measurements made in the XAFS region, in which the curvature of the mass attenuation coefficient leads to a limitation of the linearized model adopted above.

B. Finite sampling of the summation

We have tested the effect of the finite sampling of the summation of Eq. (13) over a variety of sampling frequencies and ranges. We find that full convergence for the Gaussian beam energy profile occurs when the summation is evaluated over a range of at least $r_W = 3$ FWHM with a sampling frequency of $s_{FW} = 3$ sample points per FWHM, corresponding to around two sample points per eV. The rapid convergence of this result indicates that, for the assumed Gaussian beam energy profile, the finite sampling and finite range assumptions employed in this model are both valid.

C. Choice of the model beam energy profile, $\tilde{I}_0$

We have assumed that the beam energy profile is adequately described by a Gaussian distribution of energies about the central x-ray energy, and have tested this assumption to investigate further subtleties of the shape and width of the beam energy profile. This investigation showed that the stability and convergence of the fitted bandwidth was sensitive to the asymptotic form of the beam energy profile, that is, to the tails of the distribution. In particular, the beam energy profile was *not* consistent with the asymptotic convergence of a Lorentzian distribution of energies. This was seen explicitly when testing the evaluation of the summation in Eq. (13), which does not converge with increasing range r_W. Increasing the range of the summation correlated to a decrease in the fitted bandwidth of the beam due to the increased and nonconvergent contributions from the tails of the distribution.

A similar result was reported by Parratt *et al.* [54] when attempting to correct ''thickness effects.'' Using a laboratory source, and guided by perfect crystal diffraction theory, they attempted to employ a Lorentzian beam energy profile with wide tails. These authors found by trial and error that the thickness effect resulting from a Lorentzian beam energy profile would not converge due to contributions at energies separated from the central energy by even 100 FWHM.

Parratt *et al.* thus observed that, with reasonable monochromation and collimation, an experimental cutoff was necessary, and that there must be a much sharper reduction of intensity in the tails of the beam energy profile. They employed a number of alternative tail profiles in an attempt to produce a convergent result, but were unable to arrive at any solid conclusions on this matter. Our impression is that the asymptotic form of the beam energy profile measured in our experiment (with reduced divergence and higher collimation than that of Parratt *et al.*) is either sharply truncated by the geometry of the experiment or that it is more like a Gaussian or a Voigt profile as a result of the convolution of the source spectrum with the monochromator crystal response function and the geometry of the experiment.

Improved measurements obtained in the manner of those reported here may further resolve details of a particular beam energy profile. The value of the bandwidth derived under the assumption of a Gaussian beam energy profile is completely stable when the correction is evaluated at higher sampling frequencies and wider sampling ranges, suggesting that it is not subject to instabilities due to asymptotic behavior and that it is adequate for probing the second moment of the distribution of energies in the x-ray beam (i.e.,the bandwidth).

D. Comparison with Fourier methods: Stability versus noise and sparse sampling

The magnitude of the effect of the x-ray bandwidth on the measured mass attenuation coefficients can be predicted by use of a linearized expansion of the mass attenuation coefficient, providing that the bandwidth is small compared to the structure in the mass attenuation coefficient, so that the linearized approximation is well satisfied. Here we discuss a Fourier deconvolution technique that could be used to determine the correction to the mass attenuation coefficients directly from Eq. (5).

Equation (5) describes a convolution of the beam energy profile with the ratio of transmitted to incident intensity for each individual foil thickness. In order to use Fourier deconvolution to invert this expression, we need to treat each foil thickness separately, and then compare the results of each after deconvolution. The correct value of the bandwidth would be that which minimizes the differences between the results of measurements made with each of the foil thicknesses.

However, Fourier techniques are generally very noise sensitive, and thus high precision measurements are required for this application. The varying precisions associated with the results obtained with each foil cannot be readily included as input to the Fourier transform. Furthermore, to use Fourier theory for this deconvolution it is necessary either to make measurements on an energy grid with spacing smaller than the bandwidth of the beam or to interpolate the measured intensity ratios on this grid. An additional problem arises due to the uneven grid of energies upon which the measurements have been made, which necessitates a sensitive treatment of the Fourier transform with regard to aliasing and oversampling of regions of the spectrum where the measurement interval is very different.

While each of these complications can be overcome, these complexities associated with the Fourier deconvolution have been found to give rise to numerical instability in the application described here. As a result we have followed the linearized approximation.

Porteus [55] has done some work on the use of Fourier deconvolution of an empirical ''smearing function'' and the statistical optimizations associated with this approach. However, the use of multiple datasets (one for each foil) with differing inherent precisions (resulting from the use of foils of very different thickness) makes his qualitative approach more difficult to apply, as discussed above. More importantly, we believe that the Fourier deconvolution approach remains significantly less transparent as to the identification of the major causes and signatures of the effect of the bandwidth of the beam than the technique presented here, where the first-order effect of the bandwidth is shown to depend directly on the gradient of the mass attenuation coefficient.

E. Average versus pointwise bandwidth determination

We have determined the average bandwidth of an x-ray beam over a small range of energies. The high precision of the determined average bandwidth, to within $\approx 2\%$ of estimated uncertainty, compared to the likely spread of the bandwidths (potentially up to about 20%, judging by the variation of the discrepancies presented in Fig. 4) is due to the number of independent data points used in the fit, and does not represent the real variation of the bandwidths of the beams. However, the bandwidth could in principle be determined at each experimental energy from measurements made with three foils.

This could be achieved by first removing the difference in the measured mass attenuation coefficients due to the use of the nominal foil thicknesses (as we have done) by forcing the measurements to agree at some energy far removed from the edge and from the XAFS structure. After establishing that there is a residual gradient-correlated deviation in the measurements (as presented in Fig. 4), these deviations could be corrected by use of Eq. (13) at each energy at which knowledge of the bandwidth was desired.

However, measurements taken with only three foils render the technique very susceptible to random fluctuations in those measurements. Perhaps the use of repeated measurements of sufficiently high quality on a larger number of foils (covering the same or an increased range of attenuation) could make it possible to determine the bandwidth accurately at each energy coinciding with an absorption edge using the procedure reported here, with the error in the pointwise determined bandwidths decreasing as the number of indepen-

dent foil thicknesses is increased.

This paper provides a proof of principle rather than a detailed investigation of the pointwise variation of the bandwidth.

VI. DISCUSSION OF RESULTS

A. Previous investigations of the bandwidth effect

Parratt *et al.* have so far provided the most thorough investigation of the bandwidth effect, which they termed the thickness effect [54]. These authors do not linearize the attenuation coefficient on the absorption curve, as was done here. The difference between the two approaches reflects the different systems studied: the authors of Ref. [54] investigated the white-line transition in KCl, which is not amenable to linearization due to the narrow and highly curved features present in this spectrum. Parratt *et al.* chose to determine the correction by forward calculation of the effect of the bandwidth, as described by Eq. (5). This time-consuming task yielded some insight into the effect of the bandwidth, including the need to truncate the Lorentzian beam energy profile, but was not considered practical for the accurate quantification of this effect.

Parratt *et al.* observed that resolution of the beam energy profile might be possible, but were unable to obtain a result without further input regarding the likely profile shape, as their system was particularly sensitive to the distribution of intensity in the tail regions of the beam energy profile. Since their observation, qualitative, ''in-principle'' measurements of the likely upper limit of the width of the beam energy profile have been made [56,57], but so far no other authors have taken up Parratt's suggestion that the thickness effect might be used to accurately determine the bandwidth of an x-ray beam.

B. Implications for critical investigations

Many critical experiments are prone to errors resulting from the use of a probe beam of finite bandwidth. Clearly, measurements of $[\mu/\rho]$ near absorption edges and of XAFS with highly oscillatory structure will be directly affected.

1. The measurement of mass attenuation coefficients

Our earlier presentation of the effect of the bandwidth has focussed on the difference between the measurements of the mass attenuation coefficient made with the thicker foils and those of the thinnest foil. This was useful for the presentation of the effect on a sufficiently sensitive scale. However, this presentation has had the unfortunate effect of masking the effect of the bandwidth on measurements.

To properly illustrate the systematic discrepancy which can be generated in the mass attenuation coefficient by the effect of the finite bandwidth of the beam, we present in Fig. 6 the percentage correction to the measured mass attenuation coefficients for each of the three foils used in this measurement. This figure shows that the bandwidth has resulted in a systematic effect for all measurements, rising to about 0.3%, 0.7%, and 1.4% for the thin, medium, and thick foils, respectively, at the energy at which the gradient of the mass attenuation coefficient first reaches its maximum value on the absorption edge.

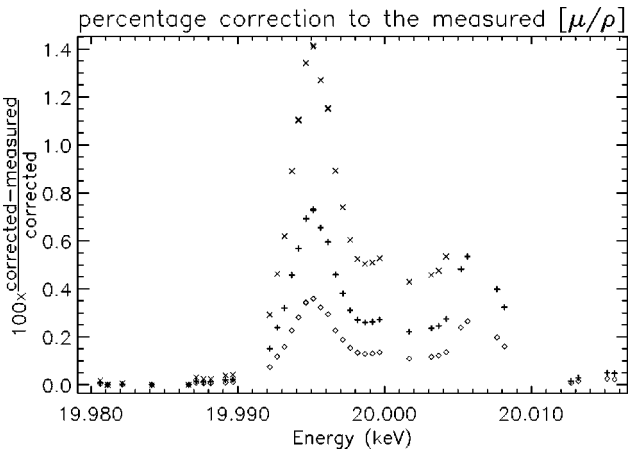

FIG. 6. The percentage correction to the measured mass attenuation coefficients of molybdenum due to the effect of the bandwidth of the x-ray beam. The correction presented here is significant for all the foil thicknesses, and contains structure which would be of interest in XAFS and XANES investigations. Symbols: ×—100 μm, +—50 μm, ◇—25 μm.

The discontinuity in these corrections to the measured values at 20.0015 keV is due to the sparse sampling of the attenuation in this region, which has resulted in a discontinuity in the value of the numerical derivative at this energy. This could be removed by use of an interpolation function (e.g.,a cubic spline), but this has not been done in the interests of presenting the calculation in a transparent manner.

The percentage correction presented in Fig. 6 contains structure which would be of interest in XAFS and XANES investigations.

2. The determination of absorption-edge energies

There are a number of definitions that can be applied to the energy location of the absorption edge. One which has gained currency recently—due to its accessibility to both theoretical prediction and experimental measurement—is that of the first point of inflection on the absorption edge.

Experimentally, this absorption-edge position is usually determined to be the location of the first peak in the first (numerical) derivative of the absorption spectrum. According to some very accurate measurements reported in the literature [58], this peak is very sharp, and one might thus expect the edge-energy to be well defined.

However, at the absorption edge, where the linearization of the attenuation coefficient is certainly valid, the correction to the absorption spectrum is proportional to the gradient of the absorption curve. Thus, the correction is greatest at the point of steepest ascent, which coincides with the first point of inflection. Effects of the bandwidth have thus the potential to shift the energy of the observed point of inflection to lower energies, with the magnitude of the shift increasing with the thickness of the foil used to make the measurement. Investigations using the absorption-edge location for the calibration of x-ray energies must therefore allow for the fact

that the measurements will also be affected by the finite bandwidth of the beam. Not correcting for the bandwidth implies that a systematic error in the calibrated energy of the order of the bandwidth of the beam must be accepted.

To provide an example, the gradient of the weighted mean of the mass attenuation coefficient shown in Fig. 2 shows how readily the absorption-edge energy location may be determined. However, a similar determination of the absorption-edge location using the results obtained only with the thickest foil (and before the correction for the effect of the finite beam bandwidth) lowers the determined energy by ≈ 0.5 eV compared to that obtained with the thinnest foil.

Interestingly, the measurements presented here can be used to determine the energy location of the absorption-edge of molybdenum. The first point of inflection of the mass attenuation coefficients in the corrected results occurs at an energy of $19\,995.0\ \text{eV} \pm 0.3\ \text{eV}$, where the error represents our ability to determine the location of the first point of inflection. The energy scale of these measurements was calibrated by measuring the locations of a number of reflections from the hhh planes of a large, perfect germanium single crystal at a number of different energies throughout the course of the experiment. These measured energies were then used to calibrate the recorded monochromator angles, which were then interpolated for all experimental monochromator angles. This has resulted in the calibration of the energies of the x-ray beam presented on the abscissa of all plots of this paper. The estimated error of the absolute value of the calibrated energies in the neighborhood of the absorption edge of molybdenum is of the order of 3 eV. We thus report a measurement of the location of the first point of inflection of the absorption edge of molybdenum with the result $19\,995\ \text{eV} \pm 3\ \text{eV}$, with the observation that the dominant source of uncertainty is due to the inaccuracies of the absolute determination of the energy of the x-ray beam. This result is not inconsistent with the result obtained by Kraft *et al.* [58], who report a value of $20\,000.36\ \text{eV} \pm 0.02\ \text{eV}$, differing from it by about 1.7 times our standard deviation. In their study, Kraft *et al.* have minimized the effect of the bandwidth by applying further monochromation to the beam, thus reducing both the bandwidth and the intensity of the beam by a few orders of magnitude. We generally agree with their conclusion that they have largely removed the effect of the bandwidth from their measurements, although we cannot comment on whether this has been achieved to the level of accuracy claimed.

3. XAFS investigations

Since the article of Parratt *et al.*, the term thickness effects has been expanded to refer more generally to any systematic effect on the measured mass attenuation coefficient that can be probed by varying the thickness of the foil used to make the measurement [59]. These effects include the presence of harmonic components in the x-ray beam, sample roughness, pinhole leakage, as well as bandwidth [54,59–64]. Refinement of the treatment of contributing factors to the thickness effects has the potential to provide powerful, quantitative probes of the spectral properties of x-ray beams, as demonstrated elsewhere with reference to the presence of harmonic components in the x-ray beam [65]. As a result of such investigations, the operational qualities of such beams, used by many scientists on a daily basis, can be investigated and addressed directly.

While thickness effects have attracted some attention in the fields of XAFS and attenuation, treatments of these effects have tended to be approximate or semiempirical at best. For instance, some analyses have defined an effective ''leakage fraction'' of ''any transmitted radiation unaffected by changes in $\Delta\mu$ (the true absorption step height)'' [60]. Our understanding of the effect of the bandwidth of the beam suggests that this interpretation of the data is qualitatively incorrect as it denies the effect due to the distribution of energies in the central region (in the neighborhood of the central energy), and concentrates on effects in the below-edge (tail of the beam energy profile) region only. We have shown here that effects resulting from the central distribution can be dominant; ignoring them is likely to yield questionable results.

Pease [66] has previously noted that the bandwidth effect does not disappear in the limit of zero thickness. However, his analysis is qualitatively different from the analysis presented here, dealing with effects related to the tails of the beam energy profile. Here the central part of the beam energy profile actually gives rise to an effect on the measured mass attenuation coefficients.

Thus, the bandwidth must be determined in order to properly measure an XAFS spectrum. Once the bandwidth has been determined, preferably by making measurements on a number of thicknesses of foil in the edge region, it can be deconvolved from the measured XAFS spectrum to recover the desired information.

4. Critical absorption

The principle of critical absorption is relatively simple: on the absorption edge, the absorption coefficient changes by up to 400% over a very narrow energy range, possibly about 0.1% of the x-ray energy. In this region, it is argued, even a relatively poor determination of the absorption of a characteristic x-ray falling on the edge will provide accurate knowledge about the energy of that x-ray. The technique of critical absorption is a clever technique enabling high resolution energy determinations to be performed, especially when the edge energy is known from other experiments. It has been applied in the determination of kaonic [67] and muonic [68] masses, and can in principle be used to determine the energy of any emission line or x ray energy that happens to coincide with an absorption edge of another material.

In order to implement the technique of critical absorption, it is necessary to obtain a calibration curve for the absorption edge in question. This can sometimes be obtained from existing tabulations, or may need to be explicitly measured. However, the technique will be compromised when, as will generally be the case, the calibration curve is measured with a beam whose bandwidth differs significantly from that of the emission line. In such cases, information will be incorrectly transferred from the calibration curve to the emission line. This source of systematic error has in general not been appreciated and can be dominant in such investigations.

The solution of this problem is to measure the absorption edge accurately and carefully in a separate experiment, correcting for the bandwidth involved, and to determine the energy of the emission line only after a similar correction for the bandwidth is made.

VII. CONCLUSION

The bandwidth of an x-ray beam is an important feature whose exact value is difficult to establish. We show that on the absorption edge, where the gradient of the absorption is large, it is possible to observe the effect of the bandwidth upon the attenuation of two or more absorbers of diverse thickness. Systematic differences between the measured attenuations of these absorbers are interpreted by a Taylor-series inversion of an equation which takes into explicit account the energy profile of the x-ray beam.

We demonstrate the technique by utilizing attenuation measurements of molybdenum on and in the vicinity of the absorption edge. We show that an x-ray beam produced by an undulator insertion device, monochromated by double reflection from the 311 planes of a silicon monochromator, whose second set of planes was slightly detuned to minimize harmonic contributions, is consistent with a Gaussian-shaped energy distribution which has an average FWHM bandwidth of $1.57\ \text{eV} \pm 0.03\ \text{eV}$.

An important advantage of the on-edge absorption technique for determining the bandwidth is the fact that it requires no knowledge of the x-ray optics of the beam and characterizes the beam after its passage through optical elements, slits, the monochromator, and after detuning. Once suitable absorbers are selected, the required attenuation measurements are straightforward and their interpretation to yield the bandwidth routine.

We find it remarkable that out of a synchrotron spectrum extending over more than 60 keV, the region in which the bandwidth can be probed extends over about 20 eV, and the typical bandwidth is of the order of 2 eV. Fortunately, the use of other absorbing materials offers a wide selection of other energies sensitive to the x-ray bandwidth. The distribution of the absorption-edge energies across the x-ray spectrum allows the selection of absorbing materials to be optimized for a given experimental investigation.

The bandwidth of the x-ray beam has a significant impact on the measurement of mass attenuation coefficients, absorption-edge energy locations, and XAFS spectra. We indicate ways by which these effects can be corrected. It is likely that proper correction for the effect of the bandwidth will reveal new structural detail in the measurement of XANES, due to the high attenuation gradient associated with these measurements, and in quantitative XAFS and white-line studies, due to the combination of the high attenuation gradient and curvature associated with these studies.

ACKNOWLEDGMENTS

We wish to acknowledge the assistance of B.B. Dhal of the University of Melbourne in performing the experiment underlying this investigation. We further acknowledge the assistance of our collaborators at the Advanced Photon Source: D.J. Cookson of CHEM-MAT-CARS, W.-K. Lee and A. Mashayekhi of SRI-CAT, and M. Beno and the staff of BESSRC-CAT. This work was supported by the Australian Synchrotron Research Program, which is funded by the Commonwealth of Australia under the Major National Research Facilities Program. Use of the Advanced Photon Source was supported by the U.S. Department of Energy, Basic Energy Sciences, Office of Energy Research, under Contract No. W-31-109-Eng-38. One of us (M.d.J.) wishes to acknowledge the Australian Research Council for their support.

[1] W. Parrish, M. Hart, T.C. Huang, and M. Bellotto, Adv. X-Ray Anal. **30**, 373 (1988).
[2] B. Rousseau, S.T. Maes, and A.T.H. Lenstra, Acta Crystallogr., Sect. A: Found. Crystallogr. **56**, 300 (2000).
[3] S.K. Sinha, Acta Phys. Pol. A **89**, 219 (1996).
[4] P. Boher, P. Houdy, and C. Schiller, J. Appl. Phys. **68**, 6133 (1990).
[5] B.E. Chapman *et al.*, Magn. Reson. Med. **37**, 519 (1997).
[6] G. Wang and M.W. Vannier, Med. Phys. **24**, 373 (1997).
[7] K. Ueda, J. Phys. B **36**, R1 (2003).
[8] T. Higuchi *et al.*, Phys. Rev. B **65**, 033201 (2001).
[9] C.T. Chantler *et al.*, Phys. Rev. A **62**, 042501 (2000).
[10] J. Ladell, A. Zagofsky, and S. Pearlman, J. Appl. Crystallogr. **8**, 499 (1975).
[11] J.I. Langford, J. Appl. Crystallogr. **15**, 315 (1982).
[12] J.A. Bearden and A. Henins, Rev. Sci. Instrum. **36**, 334 (1965).
[13] T. Fukomori and K. Futagami, Jpn. J. Appl. Phys., Part 1 **27**, 442 (1988).
[14] A.J.C. Wilson, Br. J. Appl. Phys. **16**, 665 (1965).
[15] J.S. Thomsen and Y. Yap, J. Res. Natl. Bur. Stand., Sect. A **72A**, 187 (1968).
[16] R.D. Deslattes and A. Henins, Phys. Rev. Lett. **31**, 972 (1973).
[17] S. Grosswig, K.-H. Jackel, and R. Kittner, Cryst. Res. Technol. **21**, 133 (1986).
[18] J. Hartwig and S. Grosswig, Phys. Status Solidi A **115**, 369 (1989).
[19] E. Galdecka, J. Appl. Crystallogr. **32**, 827 (1999).
[20] G. Hölzer, M. Fritsch, M. Deutsch, J. Härtwig, and E. Förster, Phys. Rev. A **56**, 4554 (1997).
[21] S. Galambosi *et al.*, Phys. Rev. A **67**, 022510 (2003).
[22] M. Deutsch *et al.*, Phys. Rev. A **51**, 283 (1995).
[23] J. Perel and R.D. Deslattes, Phys. Rev. B **2**, 1317 (1970).
[24] T. Matsushita, J. Appl. Crystallogr. **7**, 254 (1974).
[25] D. McCammon *et al.*, Nucl. Instrum. Methods Phys. Res. A **436**, 205 (1999).
[26] M. Renninger, Acta Crystallogr., Sect. A: Cryst. Phys., Diffr., Theor. Gen. Crystallogr. **31**, 42 (1975).
[27] R. Teworte and U. Bonse, Phys. Rev. B **29**, 2102 (1984).

[28] P.L. Cowan, Nucl. Instrum. Methods Phys. Res. A **222**, 46 (1984).
[29] S.M. Owens, R.D. Deslattes, and J. Pedulla, Adv. X-Ray Anal. **43**, 254 (2000).
[30] C.F. Majkrzak *et al.*, Physica A **241**, 1101 (1998).
[31] M. Deutsch and M. Hart, Phys. Rev. B **26**, 5558 (1982).
[32] P.-A. Raboud, J.-Cl. Dousse, J. Hoszowska, and I. Savoy, Phys. Rev. A **61**, 012507 (1999).
[33] C.T. Chantler, Z. Barnea, C.Q. Tran, J.B. Tiller, and D. Paterson, Opt. Quantum Electron. **31**, 495 (1999).
[34] C.T. Chantler and Z. Barnea, J. Phys.: Condens. Matter **11**, 4087 (1999).
[35] C.T. Chantler, Radiat. Phys. Chem. **55**, 231 (1999).
[36] C.T. Chantler, J. Phys. Chem. Ref. Data **29**, 597 (2000).
[37] C. Li, M. Pompa, A.C. Castellano, S. Della Longa, and A. Bianconi, Physica C **175**, 369 (1991).
[38] D. Sayers, E. Stern, and F. Lytle, Phys. Rev. Lett. **27**, 1204 (1971).
[39] J. Guo *et al.*, Phys. Rev. B **41**, 82 (1990).
[40] R. Stumm von Bordwehr, Ann. Phys. (Paris) **14**, 377 (1989).
[41] T. Yokoyama, N. Kosugi, and H. Kuroda, Chem. Phys. **103**, 101 (1986).
[42] Y.-J. Zhu, I. Coulthard, and T.K. Sham, J. Synchrotron Radiat. **6**, 529 (1999).
[43] C.T. Chantler *et al.*, Phys. Rev. A **64**, 062506 (2001).
[44] J.H. Beaumont and M. Hart, J. Phys. E **7**, 823 (1974).
[45] U. Bonse, G. Materlik, and W.J. Schröder, J. Appl. Crystallogr. **9**, 223 (1976).
[46] D.C. Creagh and J.H. Hubbell, Acta Crystallogr., Sect. A: Found. Crystallogr. **43**, 102 (1987).
[47] D.C. Creagh and J.H. Hubbell, Acta Crystallogr., Sect. A: Found. Crystallogr. **46**, 402 (1990).
[48] E.B. Saloman, J.H. Hubbell, and J.H. Scofield, At. Data Nucl. Data Tables **38**, 1 (1988).
[49] J.H. Hubbell, J.S. Coursey, J. Hwang, and D.S. Zucker, *Bibliography of Photon Total Cross Section (Attenuation Coefficient) Measurements (Version 2.3)* (National Institute of Standards and Technology, Gaithersbug, MD, 2004), p. 1907. Available at: http://physics.nist.gov/photoncs
[50] C.T. Chantler, C.Q. Tran, D. Paterson, Z. Barnea, and D.J. Cookson, X-Ray Spectrom. **29**, 449 (2000).
[51] C.T. Chantler, C.Q. Tran, D. Paterson, D.J. Cookson, and Z. Barnea, X-Ray Spectrom. **29**, 459 (2000).
[52] M.D. de Jonge, Z. Barnea, C.T. Chantler, and C.Q. Tran (unpublished).
[53] F.B. Hildebrand, *Introduction to Numerical Analysis* (McGraw-Hill, New York, 1956).
[54] L.G. Parratt, C.F. Hempstead, and E.L. Jossem, Phys. Rev. **105**, 1228 (1957).
[55] J.O. Porteus, J. Appl. Phys. **33**, 700 (1962).
[56] B.X. Yang *et al.*, Rev. Sci. Instrum. **63**, 1355 (1992).
[57] B.X. Yang *et al.*, Nucl. Instrum. Methods Phys. Res. A **316**, 422 (1992).
[58] S. Kraft, J. Stümpel, P. Becker, and U. Kuetgens, Rev. Sci. Instrum. **67**, 681 (1996).
[59] E.A. Stern, S.M. Heald, and B. Bunker, Phys. Rev. Lett. **42**, 1372 (1979).
[60] S.M. Heald and E.A. Stern, Phys. Rev. B **16**, 5549 (1977).
[61] D.M. Pease, L.V. Azároff, C.K. Vaccaro, and W.A. Hines, Phys. Rev. B **19**, 1576 (1979).
[62] E.A. Stern and K. Kim, Phys. Rev. B **23**, 3781 (1981).
[63] N.V. Bausk, S.B. Erenburg, and L.N. Mazalov, J. Synchrotron Radiat. **6**, 268 (1999).
[64] D.C. Koningsberger and R. Prins, *X-ray Absorption: Principles, Applications, Techniques of EXAFS, SEXAFS, and XANES* (Wiley, New York, 1988).
[65] C.Q. Tran *et al.*, X-Ray Spectrom. **32**, 69 (2003).
[66] D.M. Pease, Appl. Spectrosc. **30**, 405 (1976).
[67] S. Devons, G. Gidal, L.M. Lederman, and G. Shapiro, Phys. Rev. Lett. **5**, 330 (1960).
[68] G.K. Lum *et al.*, Phys. Rev. D **23**, 2522 (1981).